

**Climate impact
assessment tool:
AirClim**

V. Grewe and A. Stenke

A strategy for climate evaluation of aircraft technology: an efficient climate impact assessment tool – AirClim

V. Grewe and A. Stenke

Deutsches Zentrum für Luft- und Raumfahrt, Institut für Physik der Atmosphäre,
Oberpfaffenhofen, 82230 Wessling, Germany

Received: 9 August 2007 – Accepted: 13 August 2007 – Published: 17 August 2007

Correspondence to: V. Grewe (volker.grewe@dlr.de)

Title Page

Abstract

Introduction

Conclusions

References

Tables

Figures

⏪

⏩

◀

▶

Back

Close

Full Screen / Esc

Printer-friendly Version

Interactive Discussion

Abstract

Climate change is a challenge to society and to cope with requires assessment tools which are suitable to evaluate new technology options with respect to their impact on climate. Here we present AirClim, a model which comprises a linearisation of the processes occurring from the emission to an estimate in near surface temperature change, which is presumed to be a reasonable indicator for climate change. The model is designed to be applicable to aircraft technology, i.e. the climate agents CO₂, H₂O, CH₄ and O₃ (latter two resulting from NO_x-emissions) and contrails are taken into account. It employs a number of precalculated atmospheric data and combines them with aircraft emission data to obtain the temporal evolution of atmospheric concentration changes, radiative forcing and temperature changes. The linearisation is based on precalculated data derived from 25 steady-state simulations of the state-of-the-art climate-chemistry model E39/C, which include sustained normalised emissions at various atmospheric regions. The results show that strongest climate impacts from ozone changes occur for emissions in the tropical upper troposphere (60 mW/m²; 80 mK for 1 TgN emitted), whereas from methane in the middle tropical troposphere (−2.7% change in methane lifetime; −30 mK per TgN). The estimate of the temperature changes caused by the individual climate agents takes into account a perturbation lifetime, related to the region of emission. A comparison of this approach with results from the TRADEOFF and SCENIC projects shows reasonable agreement with respect to concentration changes, radiative forcing, and temperature changes. The total impact of a supersonic fleet on radiative forcing (mainly water vapour) is reproduced within 5%. For subsonic air traffic (sustained emissions after 2050) results show that although ozone-radiative forcing is much less important than that from CO₂ for the year 2100. However the impact on temperature is of comparable size even when taking into account temperature decreases from CH₄. That implies that all future measures for climate stabilisation should concentrate on both CO₂ and NO_x emissions. A direct comparison of super- with subsonic aircraft (250 passengers, 5400 nm) reveals a 5 times higher climate impact of

ACPD

7, 12185–12229, 2007

Climate impact assessment tool: AirClim

V. Grewe and A. Stenke

Title Page

Abstract

Introduction

Conclusions

References

Tables

Figures

◀

▶

◀

▶

Back

Close

Full Screen / Esc

Printer-friendly Version

Interactive Discussion

EGU

supersonics.

1 Introduction

Air traffic has the potential to grow over-proportional compared to other transport sectors. Its specific climate impact, i.e. relative to fuel consumption is larger than for other sectors (Fuglestad et al., 2007¹). One reason is the higher altitude of the emission, which leads to longer atmospheric residence times, particularly in the case of NO_x emissions and its chemical products (ozone, methane).

Therefore, there is a need to develop technical and operational options to reduce the impact from air traffic emissions on climate and to provide tools to reliably assess these impacts, or at least to provide some metrics for various technology options within a range of uncertainty.

In this context it is important to note that a simple metric based on fuel consumption or emission indices insufficiently describes the total climate impact. The dependency of the strength of the impact on altitude and region cannot be described by such metrics. For example, contrail formation depends on aircraft design aspects (propulsion efficiency), water vapour emission (directly related to fuel consumption), but also and equally important on local atmospheric conditions (Schumann et al., 2000).

We concentrate on near surface temperature changes as a metric for climate change, as we think it is the most suitable metric for our purpose. Other metrics, e.g. global warming potentials, have been widely discussed (Fuglestad et al., 2003; Shine et al., 2005) and a time-integrated radiative forcing including its efficacy has been chosen to be appropriate. Sausen and Schumann (2000) presented a linear response model, which allows estimates of near surface temperature changes based on precalculated radiative forcings, which are combined with a transient emission scenario to take into

¹Fuglestad, J., Berntsen, T., Myhre, G., Rypdal, K., and Skeie, R.: Climate forcing from the Transport Sectors, PNAS, submitted, 2007.

**Climate impact
assessment tool:
AirClim**

V. Grewe and A. Stenke

Title Page

Abstract

Introduction

Conclusions

References

Tables

Figures

◀

▶

◀

▶

Back

Close

Full Screen / Esc

Printer-friendly Version

Interactive Discussion

account accumulation effects, e.g. for CO₂. This means that the climate response of a given radiative forcing is linearised in this approach to calculate the associated temperature change. Response functions were derived on the basis of an ocean-atmosphere model.

5 Here we present an assessment tool, which is an extension to the linear response model described in [Sausen and Schumann \(2000\)](#). The extension comprises a linearisation of the relation between emissions of CO₂, NO_x and H₂O and impacts on atmospheric composition related to carbon dioxide, ozone, methane, water vapour, and contrails. Note that in our approach spatially resolved emissions are taken into account in contrast to [Sausen and Schumann \(2000\)](#) who concentrated on annual global values. Hence, the input to the AirClim model are 3-D aircraft emission data, precalculated atmospheric data and some parameters describing the overall evolution of air traffic and some background concentrations, which are all converted into a timeseries of near surface temperature changes.

10 A detailed description of the methodology is given in Sect. 2, followed by a description of the atmospheric input data, i.e. a description of the simulation results employing idealised emission scenarios. These are forming the basis for the linearisation of chemical and radiative responses. A validation of the chemical and radiative responses is given in Sect. 4 by comparing them to detailed climate-chemistry simulations. In Section 5 some applications are presented with respect to sub- and supersonic air traffic.

2 Methodology

2.1 Overview

25 An overview of the methodology is given in Fig. 1. The main part of the model AirClim is indicated in blue, showing the functional chain from emissions (yellow) and precalculated atmospheric input data (rose) to the resulting global mean near surface temperature change, which is described in detail, below. A more detailed description of the

**Climate impact
assessment tool:
AirClim**

V. Grewe and A. Stenke

Title Page

Abstract

Introduction

Conclusions

References

Tables

Figures

⏪

⏩

◀

▶

Back

Close

Full Screen / Esc

Printer-friendly Version

Interactive Discussion

precalculated atmospheric input data is given in the next section. These data describe the Jacobian of the atmosphere-chemistry system with respect to emissions of CO₂, NO_x, and H₂O, or in other words the atmospheric sensitivity to regional emissions.

2.2 Precalculated input data

5 In the first step we define emission regions with a normalised (=equal for all regions) emission strength (in mass mixing ratios per time). Then, in a second and third step chemical perturbations and radiative forcing of CO₂, ozone, methane, water vapour, and contrails are calculated applying a state-of-the-art climate-chemistry model (here: E39/C). These results will then be linearly combined with emission perturbation data to
10 obtain perturbation patterns of chemical species and the associated radiative forcing (Sect. 2.4).

2.2.1 Idealised emission regions

Emission regions are presented in Fig. 2 (see also Tables 1 and 2). We have defined areas for three potential supersonic cruise levels (SSCL). Since the impact will depend
15 on the geographical distribution, also 4 latitudinal bands are taken into account. Additionally, three levels for subsonic air traffic are included to represent take-off, climb and cruise. This leads to 24 regions.

Since we mainly concentrate on supersonic (stratospheric) air traffic, we limited the number of flight levels to a subsonic fleet. However, the methodology is set-up in a way
20 that additional emission regions can easily be added, refining the methodology.

For each of the regions a uniform emission is defined, which is derived from the SCENIC dataset: At 50° N the zonally integrated fuel consumption varies between 500 and 2000×10⁻⁹ kg/s/m² and 200 and 500×10⁻⁹ kg/s/m² for subsonic (≈12 km) and supersonic cruise levels (18–19 km), respectively. This relates to 62–247×10⁻¹⁵ kg/kg/s and 77–192×10⁻¹⁵ kg/kg/s, respectively. Mean values are chosen to represent these
25 ranges (Table 3).

**Climate impact
assessment tool:
AirClim**

V. Grewe and A. Stenke

Title Page

Abstract

Introduction

Conclusions

References

Tables

Figures

◀

▶

◀

▶

Back

Close

Full Screen / Esc

Printer-friendly Version

Interactive Discussion

2.2.2 Chemical composition

For each of the idealised emission regions, a climate-chemistry simulation is performed employing a normalised emission of nitrogen oxides and water vapour to obtain the chemical response of an emission in that region. We applied the climate-chemistry model E39/C (Hein et al., 2001), in which we accounted for full Lagrangian transport (ATTILA, Reithmeier and Sausen, 2002) of all species including water vapour and cloud water, which significantly improved the representation of stratospheric water vapour and temperatures (Stenke et al., 2007²). E39/C consists of the troposphere-stratosphere climate model ECHAM4.L39(DLR) (E39, Land et al., 1999) and the troposphere-stratosphere chemistry module CHEM (Steil et al., 1998). Recently, a number of revisions were released (Dameris et al., 2005). An overview of validation activities is given in Grewe (2006).

The experimental set-up comprises a steady-state simulation (time-slice) for the year 2050, which means boundary conditions, like background CO₂, CH₄, N₂O, and CFC concentrations, emissions of NO_x from industry, biomass burning, transport, and soils and sea surface temperatures represent predicted conditions for the year 2050. They are prescribed according to IPCC (2001) or are taken from coupled ocean-atmosphere model simulations. Latter applies for ocean temperatures. Background aircraft emissions include subsonic aircraft (SCENIC-database, scenario S4, Marizy et al. (2007)³, see also Table 4). This defines a base case simulation. Twenty-four perturbation simulations, one for each emission region, are performed including an additional constant emission of NO_x and H₂O (see above). After a spin-up time, five consecutive years are calculated in order to obtain annual mean changes.

Figure 3 shows exemplarily for the two emission regions SSCL-H/Pole (top) and

²Stenke, A., Grewe, V., and Ponater, M.: Lagrangian transport of water vapor and cloud water in the ECHAM4 GCM and its impact on the cold bias, *J. Climate*, revised, 2007b.

³Marizy, C., Rogers, H., and Pyle, J.: The SCENIC emission database, *Atmos. Chem. Phys. Disc.*, in preparation, 2007.

Title Page

Abstract

Introduction

Conclusions

References

Tables

Figures

◀

▶

◀

▶

Back

Close

Full Screen / Esc

Printer-friendly Version

Interactive Discussion

SSCL-M/Pole (bottom) changes in water vapour (left), nitrogen oxides (NO_y , mid), and ozone (right). Water vapour (left) shows an increase of around 150 ppbv and 100 ppbv at high northern latitudes for high and mid supersonic cruise levels, which corresponds to an increase of around 9 and 6%, respectively. In the stratosphere the loss processes are similar for water vapour and nitrogen oxides (NO_y) perturbations, therefore the lifetimes and hence the change pattern of the perturbations are almost identical in the stratosphere. The impact on ozone (Fig. 3, right) strongly depends on altitude and latitude of the perturbation. The climate-chemistry model E39/C shows a transition from ozone increase to ozone decrease roughly 4 km above the tropopause for the case of the mid supersonic cruise level (bottom). Ozone decrease is the stronger the higher the emissions occurs (top). The decrease in stratospheric ozone is compensated by a tropospheric increase as seen in the simulation for the mid supersonic cruise level (bottom).

2.2.3 Contrail coverage

Contrail coverage is calculated by folding the potential contrail coverage (Fig. 6) with flight data. The potential contrail coverage is the maximum possible coverage in the case that aircraft are flying everywhere at any time. It is calculated with E39/C including a parametrisation for line-shaped contrails (Ponater et al., 2002). According to Sausen et al. (1998) a linear scaling including a non-physical parameter (see also below) folded with the flown distance provides the actual coverage. Contrails may occur in regions, which are both cold and humid enough so that additional water vapour leads to cloud formation (Fig. 6). These regions are limited to the tropopause area (see thick line for the location of the tropopause).

2.2.4 Radiative forcing of idealised perturbation scenarios

To each of the perturbation scenarios the stratospheric adjusted radiative forcing is calculated for ozone and water vapour changes, using the E39 model. Simulations

Title Page

Abstract

Introduction

Conclusions

References

Tables

Figures

◀

▶

◀

▶

Back

Close

Full Screen / Esc

Printer-friendly Version

Interactive Discussion

are performed with a length of 15 months which include the annual mean perturbation patterns derived from the chemical composition change simulations (2.2.2), following the methodology by [Stuber et al. \(2001\)](#). The annual mean is calculated based on the last 12 months.

5 2.2.5 Climate sensitivity and efficacies

Although changes in chemical species may lead to the same radiative forcing their impact on climate (temperature) may differ significantly ([Stuber et al., 2001](#); [Joshi et al., 2003](#)). This relationship is expressed in terms of climate sensitivity, i.e. the change in near surface temperature relative to a normalised radiative forcing (1 W/m^2) or in terms of efficacies ([Hansen et al., 2005](#)), which are these climate sensitivity parameters normalised to that of CO_2 . Efficacies for a variety of climate agents are taken from literature ([Ponater et al., 2005, 2006](#)). Those values are derived from long-term steady-state simulations applying a coupled ocean-atmosphere model (here: E39 coupled to a mixed layer ocean model) to a well defined radiative forcing. The ratio of the temperature perturbation to the radiative forcing gives the climate sensitivity for that kind of perturbation. The values used are identical to those in [Grewe et al. \(2007\)](#) (their Table 7).

2.3 Emission data

The aim of the application of the model AirClim is to compare technological options for aircraft with respect to a climate change metric and a UV-change metric. The latter is only important for supersonic transport and can be omitted for subsonic applications. Hence, at least three emission dataset are needed: A base case scenario and two scenarios which include perturbations or technological options to the base case and which are aimed to be intercompared. In principle two approaches are applicable. If enough knowledge is available on the future development of the considered fleet, then 3-D distributions of emissions of the base case and the perturbations can be

**Climate impact
assessment tool:
AirClim**

V. Grewe and A. Stenke

Title Page

Abstract

Introduction

Conclusions

References

Tables

Figures

◀

▶

◀

▶

Back

Close

Full Screen / Esc

Printer-friendly Version

Interactive Discussion

used, i.e. this refers to the case of normal passenger aircraft, where present traffic is well known and estimates for future traffic exist (e.g. Marizy et al., 2007³). However, in the case of business jets, even nowadays traffic is only poorly known and future developments are even less explored. In this case, we suggest to take an arbitrary base case (e.g. Marizy et al., 2007³). For a perturbation scenario emissions are added to the base case. For these perturbations city pairs for flight connections can be chosen, whose flight paths are somehow equally distributed over the globe. These city pairs are used for all technology options considered. A linear combination (to differently weight each region) of the emissions along the flight paths is used as an estimate for the considered fleet emissions. The weighting of the regions, i.e. the linear combination is somehow arbitrary and therefore object to an uncertainty analysis (see below). In all cases at least 3 three-dimensional emission datasets are considered and serve as input to the model AirClim.

In addition, a general temporal development of the base case air traffic has to be considered to take into account accumulation effects, e.g. of CO₂ emissions. Further, a year has to be defined, when the technology options are taken in service and a year (T^{const}) for which the 3-D emission data discussed above are representative (here: $T^{\text{const}}=2050$). For the present investigation, we suggest to keep the emissions constant for all scenarios after this date. One reason is that the composition change simulations (see Sect. 2.2.2) are 5 year steady-state simulations and hence are based on constant emissions. Further this date is far in the future (2050) so that projections are highly uncertain, anyway. However, other scenarios may well be taken into account. In any case, the impact is somehow limited, since all scenarios are compared to the base case in the end. Figure 7 shows an example of emission scenarios, which are used in the validation Section (Sect. 4).

2.4 Linear response model: AirClim

The model AirClim (see Fig. 1) combines the precalculated (Sect. 2.2) altitude and latitude dependent perturbations with the emission data (Sect. 2.3) to obtain a metric

**Climate impact
assessment tool:
AirClim**

V. Grewe and A. Stenke

Title Page

Abstract

Introduction

Conclusions

References

Tables

Figures

◀

▶

◀

▶

Back

Close

Full Screen / Esc

Printer-friendly Version

Interactive Discussion

for climate change.

2.4.1 Transient emissions, concentration and radiative forcing changes

The development of the base case CO₂ emission and concentration changes are defined by input parameters. CO₂ emissions of the perturbation scenarios are calculated by integrating the emissions along the flight paths, which are representative for the year T^{const} . They are exponentially interpolated between the time of in-service and T^{const} . The resulting changes in the concentration of CO₂ are calculated using a constant lifetime of 100 years.

The concentration changes of all other species are calculated for a time $T^{\text{const}} + \tau_{\text{species}}$ with τ_{species} the lifetime of the respective species. It takes into account that the precalculated concentration patterns are derived from steady-state simulations. In detail, the concentration changes of a species C^{species} (e.g., ozone and water vapour) for a perturbation scenario are calculated by folding the emissions along the flight paths with the precalculated scenarios:

$$C^{\text{species}} = \frac{1}{T} \int_0^T \frac{E^{\text{species}}(t)}{X} \sum_k \frac{\epsilon_k(t) C_{id}^{\text{species}}(i_k, j_k)}{M(i_k, j_k)} dt, \quad (1)$$

where $\epsilon_k(t)$ ($k = 1, \dots, 4$) are weights for the four surrounding emissions regions (i_k, j_k) (i_k =latitude, j_k =pressure level) at a certain point of the flight path, $C_{id}^{\text{species}}(i_k, j_k)$ the concentration change in [kg/kg] from the idealised scenario (i_k, j_k) (Tables 1 and 2), $M(i_k, j_k)$ the respective mass of air in the idealised emission region in [kg], and $E^{\text{species}}(t)$ the emission of species in [kg/s]. Note that C^{species} and $C_{id}^{\text{species}}(i_k, j_k)$ are 2-dimensional fields. X is the respective normalised emission strength (Table 3). $X \times M(i_k, j_k)$ then gives the emission rate (in kg/s) in the idealised emission region.

Other quantities are derived in a similar way, e.g. the radiative forcing is derived by replacing C_{id}^{species} in Eq. (1) by the radiative forcing RF_{id}^{species} (Fig. 4c,d). Changes in methane lifetime, the lifetimes of tropospheric ozone and stratospheric quantities are

**Climate impact
assessment tool:
AirClim**

V. Grewe and A. Stenke

Title Page

Abstract

Introduction

Conclusions

References

Tables

Figures

◀

▶

◀

▶

Back

Close

Full Screen / Esc

Printer-friendly Version

Interactive Discussion

derived accordingly, considering either tropospheric or stratospheric emissions only. The 100 hPa level is used for the separation between troposphere and stratosphere. A climatological tropopause based on temperature profiles would be feasible, however emissions in the lowermost stratosphere have also a limited lifetime, which is more similar to the upper troposphere than mid stratosphere.

The change in methane is then derived by regarding the difference of two linear differential equations for background methane (C^{CH_4}) and the perturbation ($C^{\text{CH}_4} + \Delta C^{\text{CH}_4}$), which both have the same production terms and the loss differs by the change in methane lifetime, resulting in

$$\frac{d}{dt} \Delta C^{\text{CH}_4} = \frac{\delta}{1 + \delta} \tau_{\text{CH}_4}^{-1} C^{\text{CH}_4} - \frac{1}{1 + \delta} \tau_{\text{CH}_4}^{-1} \Delta C^{\text{CH}_4}, \quad (2)$$

where δ is the relative change in lifetime, τ_{CH_4} the methane lifetime (here: 9 years) and C^{CH_4} the background methane concentration, e.g. taken from IPCC (2001). A temporal evolution of the change of the methane lifetime is achieved by scaling it with normalised CO_2 emission, such that $\delta(\tau^{\text{const}} + \tau_{\text{CH}_4}) = \delta$.

The temporal evolution of concentration changes $C^{\text{species}}(t)$ of tropospheric ozone and stratospheric quantities (ozone and water vapour) is calculated by solving a simple linear differential equation taking the respective lifetime into account. Since we regard only changes relative to C^{species} at $\tau^{\text{const}} + \tau_{\text{species}}$, we scale the concentration changes so that they are 1 at that time, i.e. $C^{\text{species}}(\tau^{\text{const}} + \tau_{\text{species}}) = 1$. A proportionality is assumed between changes in methane and its radiative forcing (IPCC, 1999).

In principle changes in contrail coverage can be estimated applying the identical methodology as for ozone and water vapour, by applying Eq. (1). However, contrail occurrence is more constrained to altitudes around the tropopause (see Fig. 6), which requires a higher vertical resolution of the idealised scenarios than currently performed. Therefore, we suggest here an alternative method. The potential contrail coverage presented in Fig. 6 is used and linearly folded with data of flown distance, which leads to a 2-D contrail coverage (see also Sect. 4 and Fig. 8c, e). The advantage is that the

**Climate impact
assessment tool:
AirClim**

V. Grewe and A. Stenke

Title Page

Abstract

Introduction

Conclusions

References

Tables

Figures

◀

▶

◀

▶

Back

Close

Full Screen / Esc

Printer-friendly Version

Interactive Discussion

horizontal and vertical resolution is much better resolved with $48 \times 39 = 1872$ gridpoints compared to 24 if only the idealised scenarios are applied. Global total contrail coverage is calculated by vertical summation taking into account maximum random overlap (Manabe and Strickler, 1964). The non-physical scaling parameter $\gamma = 0.00166 \text{ s m}^2/\text{km}$ is chosen such that the global value is identical to a reference 3-D GCM simulation (see below) applying the SCENIC database. Contrail radiative forcing is calculated by applying a linear relationship between contrail coverage and radiative forcing: 6.384 W/m^2 for 100% total contrail coverage (Stenke et al., 2007⁴).

2.4.2 Temperature change

The temperature change caused by the perturbation scenarios is calculated following the approach of Sausen and Schumann (2000):

$$\Delta T = \int_{t_0}^T G(t - t') RF^*(t') dt', \quad (3)$$

with

$$G(t - t') = \alpha e^{-\frac{t-t'}{\tau}}, \text{ with} \quad (4)$$

$$\alpha = 2.246/36.8 \frac{\text{K}}{\text{a}} \text{ and } \tau = 36.8 \text{ a}$$

$$RF^*(t) = \sum_{\text{species}} \frac{RF^{\text{species}}}{RF^{\text{CO}_2}} \lambda_{\text{species}}^{\text{eff}} \frac{\Delta C_i(t)}{\iint C^{\text{species}} dp dl dt} \quad (5)$$

ΔT describes the perturbation temperature with respect to the base case, G the Green's function for the near surface temperature response and RF^* the normalised radiative forcing. Because of the small changes in the concentration, especially for

⁴Stenke, A., Grewe, V., and Pechtl, S.: Do supersonic aircraft avoid contrails?, Atmos. Chem. Phys. Discuss., 7, in preparation, 2007a.

Title Page

Abstract

Introduction

Conclusions

References

Tables

Figures

◀

▶

◀

▶

Back

Close

Full Screen / Esc

Printer-friendly Version

Interactive Discussion

CO₂, saturation effects are omitted, different to the approach by Sausen and Schumann (2000).

In order to illustrate the relationship between emission, radiative forcing and temperature change, as well as the impact of different lifetimes of atmospheric tracers, a thought experiment is given in Fig. 7. We consider an increase in emissions up to the year 2050 and switch them off afterwards (Fig. 7a). A supersonic impact scenario is taken as emission scenario, i.e. the SCENIC mixed fleet minus subsonic fleet scenario (Grewe et al., 2007) (S5–S4), where the first HSCT aircraft are in service in 2015, a second generation evolves in 2025 and the full fleet is established in 2050. Again for illustrative reasons, all time series are normalised to their maximum values. Figure 7a illustrates the relation between CO₂ emissions, radiative forcing and temperature changes. The radiative forcing from CO₂ slowly decreases after 2050, mirroring the relatively long lifetime of CO₂. Temperature increase peaks much later (around 2080) caused by the inertia of the ocean-atmosphere system.

Other species show different behaviour for radiative forcing (Fig. 7b) (and their concentration, not shown) and the associated temperature increase (Fig. 7c) according to the lifetime of the regarded species: Contrails and tropospheric ozone have shorter lifetimes, hence radiative forcing decreases more rapidly than that of stratospheric water vapour, methane and CO₂. Maximum temperature change is found for contrails and tropospheric ozone changes around 2050, whereas methane peaks around 2060 and CO₂ around 2080.

3 Atmospheric sensitivity to emissions

In order to evaluate the chemical impact of air traffic emissions 25 simulations (1 base case and 24 perturbations, see Fig. 2) with the climate-chemistry model E39/C are performed (see above) for each of the selected emission region. These precalculated data (with respect to the application of AirClim) describe the sensitivity of the atmosphere to the emission region. Since the emission regions do not have the same air mass, the

**Climate impact
assessment tool:
AirClim**

V. Grewe and A. Stenke

Title Page

Abstract

Introduction

Conclusions

References

Tables

Figures

◀

▶

◀

▶

Back

Close

Full Screen / Esc

Printer-friendly Version

Interactive Discussion

results presented in Fig. 3 are not directly intercomparable. In contrast, the lifetimes of the perturbations, i.e. the mass of the perturbation divided by the emission strength are directly intercomparable. Figure 4a shows the lifetimes of the perturbations for every emission region. For the polar region the water vapour perturbation has a lifetime of 13 months, whereas at lower altitudes the lifetime decreases to 9 and 4.3 months for the mid and low supersonic cruise altitude. At subsonic cruise levels the lifetime of a water vapour perturbation amounts to around 1 month and is less than 1 h for climb and take-off.

Changes in ozone and water vapour also have an impact on the concentration of the hydroxyl radical (OH). The reaction of OH with methane (CH₄) is the dominant tropospheric methane loss process. Although methane changes are calculated in the idealised scenarios, they do not represent the steady-state methane change, basically for two reasons. First, methane has a lifetime of around 8 to 9 years, which implies that a far longer simulation time is necessary to accurately calculate methane changes. Second, at the surface, methane is prescribed to correctly represent tropospheric methane. This offsets methane changes to some extent. For that reason methane loss rates from the reaction with the hydroxyl-radical (OH) are calculated and converted into a methane lifetime. Changes in this methane lifetime are deduced from the difference in the background and perturbation simulation. Additionally, a factor of 1.4 is taken into account for reductions in the loss rates due to the boundary condition (IPCC, 1999). Figure 4b shows relative changes (%) in tropospheric methane lifetime for the 24 emission regions. Two regions can be identified, where an emission of NO_x reduces methane lifetime most: The stratosphere at high supersonic cruise level, as already indicated in the results of the ozone change (see above) and the tropical troposphere (−2.7% change in methane lifetime at 500 hPa and −2.5% at 200 hPa for 1 TgN emitted), where chemistry is fast and reacts more sensitively to emissions. Minimum changes are found at tropopause levels, where chemistry is generally slow and OH formation limited by either water vapour concentration and UV irradiance.

Figures 4c, d present the results for water vapour and ozone scaled to a normalised

**Climate impact
assessment tool:
AirClim**

V. Grewe and A. Stenke

Title Page

Abstract

Introduction

Conclusions

References

Tables

Figures

⏪

⏩

◀

▶

Back

Close

Full Screen / Esc

Printer-friendly Version

Interactive Discussion

emission of 1 Pg H₂O and 1 TgN, respectively. The effects from water vapour emissions qualitatively follow the pattern of the respective lifetime (Fig. 4a) and leads to a warming independent of the location of the emissions. In the extra-tropics no sensitivity to the respective latitude of the emission is found, in contrast to ozone (Fig. 4d).

NO_x emissions show largest impact on ozone radiative forcing in the tropical upper troposphere with a large latitudinal gradient from 60 mW/m² per 1 TgN emitted to less than 5 mW/m² at higher latitudes. In contrast, NO_x emissions at high supersonic cruise altitude lead to a negative radiative forcing at mid and high latitudes and hence to a decrease of near surface temperature.

In order to intercompare the climate impact of a unit emission in the emission regions, i.e. the regional dependency of the near surface temperature change to the emission region, we have applied AirClim for the pre-defined emission regions (Fig. 2; Table 3) with a normalised emission strength. The strength of the emission is secondary, since we focus on the regional patterns. However, the ratio of water vapour emissions, i.e. fuel consumption, to NO_x emissions is important. Here we take the mean value from the SCENIC subsonic emission data (S4; EI(NO_x)=10.85 g(NO₂)/kg(fuel)). Figure 5 shows the near surface temperature change for 2100 as a function of altitude and latitude of the emission (note that we assume steady-state for the period 2050 to 2100). The temperature increase due to water vapour changes and the temperature decrease due to methane changes (Fig. 5a, c) reflect directly their lifetime pattern (Fig. 4a). The temperature changes due to water vapour and ozone (5a, b) also reflect their radiative forcing (Fig. 4c, d). Although the lifetime of methane changes is considerably larger than for ozone it does not compensate for the smaller radiative forcing. Hence ozone changes from NO_x emissions dominate the temperature change over the compensating methane effect (Fig. 5d), at least for this specific emission index of NO_x, or smaller indices. Figure 5e shows the sum of all effects. Clearly, the higher the altitude of an emission the larger is its climate impact. There is also a clear difference between tropical and extra-tropical emission locations, with a lower climate impact at high latitudes.

**Climate impact
assessment tool:
AirClim**V. Grewe and A. Stenke

Title Page

Abstract

Introduction

Conclusions

References

Tables

Figures

◀

▶

◀

▶

Back

Close

Full Screen / Esc

Printer-friendly Version

Interactive Discussion

4 Validation of the linearisation approach

The basic question is, whether linearisation of the effect of emissions on the chemical composition and contrail coverage is applicable to aircraft emissions. This is investigated by comparing results from a detailed climate-chemistry simulation (E39/C) with the results of the linearised model AirClim. In the detailed simulation, E39/C is applied to calculate ozone, water vapour and contrail cover changes and the associated radiative forcing. In the linearised approach the precalculated perturbations of the chemical composition and contrail cover as well as their respective radiative forcing are folded with the emission data set. Hence, two simulations for each model are performed, one including emissions of water vapour and nitrogen oxides from a subsonic fleet and another one, which includes emissions from a mixed sub- and supersonic fleet, where 500 subsonic aircraft are replaced by supersonics in a way that the passenger transport volume is unaffected. A more detailed discussion of the chemical impacts is given in [Grewe et al. \(2007\)](#) and a discussion of the contrail impacts in [Stenke et al. \(2007\)](#)⁴. Here we concentrate on the differences between the detailed and the linearised approach.

Figure 8 shows the results for E39/C (top) and AirClim (bottom) for the difference of the two model simulations, i.e. the impact of a partial replacement of subsonic aircraft by supersonics. Clearly, magnitude and pattern of the change in water vapour is similar in both models. Maximum values of around 300 ppbv are found in both models on the northern hemisphere at around 70 hPa, decreasing to around 30 ppbv at tropopause altitudes. However, differences occur on tropical and southern latitudes, where the water vapour enhancement is underestimated by 50% in AirClim. Clearly, the low resolution in AirClim, where the whole atmosphere is resolved by 24 gridpoints compared to 180 000 gridpoints in E39/C, leads to numerical diffusion. Note, that only radiative forcing values will further be taken into account for calculating temperature changes, which are not calculated based on the fields presented in Fig. 8, but calculated from the radiative forcing of the idealised scenarios.

Title Page

Abstract

Introduction

Conclusions

References

Tables

Figures

◀

▶

◀

▶

Back

Close

Full Screen / Esc

Printer-friendly Version

Interactive Discussion

Both models show a similar pattern in ozone changes (Fig. 8 middle column) caused by a partial substitution of subsonic air traffic. Ozone depletion peaks in the tropical stratosphere at around 10 hPa and at northern mid-latitudes at around 50 hPa. In the troposphere a distinct difference is found between northern and southern hemisphere with a decrease and increase in ozone, respectively. Absolute values of ozone changes differ only slightly between the models.

Contrail formation changes for both models are shown in Figs. 8c, f. The results for the linearised model are scaled with the non-physical parameter γ to give the same global contrail coverage (see Sect. 2.4.1) for this reference case. Note that for all other applications to emission datasets this parameter remains unchanged. The global pattern is very similar in both simulations. A decrease in contrail coverage due to the replacement of subsonic aircraft is compensated by a tropical increase in contrail coverage. Both simulations show a good agreement of the pattern, e.g. an increase in contrail coverage at some subsonic cruise levels, i.e. where supersonic aircraft fly at subsonic speed (over land).

Table 5 shows the radiative forcing from the substitution of parts of a subsonic fleet by supersonics (SCENIC S5-S4 scenario) as calculated by Grewe et al. (2007) (top) and with the AirClim model. Clearly, water vapour, the dominant climate agent in this case, is well reproduced. Other parameters, which are an order of magnitude smaller show larger deviations. In general, the more complex the chemical and physical processes are the larger are the deviations. Water vapour is mainly dynamically controlled, whereas ozone and methane are dynamically and chemically controlled. The linearisation of methane effects includes the longest functional chain among all of the species regarded.

Hence the linearisation of transport, chemistry, contrail formation and radiation is working sufficiently well. The pattern and absolute values of concentration changes are well reproduced and the total radiative forcing agrees within 3.6% between the linearised model AirClim and the non-linear climate-chemistry model E39/C.

**Climate impact
assessment tool:
AirClim**V. Grewe and A. Stenke

Title Page

Abstract

Introduction

Conclusions

References

Tables

Figures

◀

▶

◀

▶

Back

Close

Full Screen / Esc

Printer-friendly Version

Interactive Discussion

5 Climate impact of air traffic

In this section a first application of AirClim is performed with respect to subsonic and supersonic air traffic. We are focusing on the importance of CO₂ versus NO_x emissions for subsonic air traffic, a climate impact minimization for options of supersonics and the difference between sub- and supersonic transport with respect to climate change. The numerical efficiency of the linearised model facilitates the analysis of a number of air traffic scenarios, which would not be possible applying climate-chemistry models.

Although AirClim has been designed, as a first step, to be applicable to supersonic transport, it basically can be applied to all kind of 3-D emission data. However, the coarse vertical resolution in the area of subsonic transport limits its applicability, which is described in more detail below. In future, we will enhance this resolution in order to achieve a full applicability with respect to air traffic.

In our study, we concentrate on the TRADEOFF aircraft emission data (Sausen et al., 2005) for the year 2000 and the SCENIC emission data (Marizy et al., 2007³) for the years 2025 and 2050 (Table 4) since for those datasets also radiative forcing estimates are available. For the period prior to 2000 we take historical records into account (IPCC, 1999).

5.1 Subsonic air traffic: TRADEOFF and SCENIC

Table 6 shows the comparison of radiative forcing from Sausen et al. (2005), which are based on a number of model simulations, with AirClim, for the year 2000. The results obtained with AirClim are similar to those in Sausen et al. (2005) and within the range of uncertainty given therein. Differences in CO₂ may occur due to an assumption of exponential temporal interpolation between given historical values for fuel consumption, which slightly decreases the accumulation of CO₂. Larger differences occur for methane, where AirClim shows a lower sensitivity compared to the mean value in Sausen et al. Again, the values are still in the range of uncertainty.

Figures 4b, c, d show a small sensitivity of ozone and methane radiative forcing to the

Title Page

Abstract

Introduction

Conclusions

References

Tables

Figures

◀

▶

◀

▶

Back

Close

Full Screen / Esc

Printer-friendly Version

Interactive Discussion

subsonic flight altitude, whereas for water vapour the sensitivity is very large. Hence in the present state AirClim is not able to correctly represent the water vapour radiative forcing from subsonic air traffic. The vertical resolution of AirClim is not sufficient to resolve the water vapour impact at tropopause regions. To obtain reasonable values for water vapour radiative forcing from subsonic air traffic we have multiplied this value by 0.25 to overcome this deficiency for the further discussion of the temperature effects. The water vapour impact is regarded to be small for subsonic air traffic, anyway (IPCC, 1999; Sausen et al., 2005).

Figure 9a presents the temporal evolution of temperature changes derived with AirClim for the above described emission scenario. Note that again the emissions are kept constant after the year 2050 for illustration purpose. For short-term perturbations (ozone, contrails and water vapour) the temperature change reaches equilibrium in less than 100 years after the emissions are kept constant. Species with a longer atmospheric lifetime (CH_4 and CO_2) reach steady-state after around 150 years.

In Fig. 10 we compare the climate impact of CO_2 and NO_x emissions of subsonic air traffic for the year 2000, 2100, and 2250 applying the metrics radiative forcing and temperature change. Note that the year 2250 is only taken into account to represent steady-state. There is no other meaningful interpretation, since the results largely depend on the assumptions of the air traffic scenario.

For all points of time radiative forcing from CO_2 is larger than the radiative forcing of the products of NO_x emissions, i.e. ozone and the sum of ozone and methane (left three bars at each date). However, the temperature changes (right three bars at each date), ozone and methane are larger than for CO_2 in the year 2000. This is a consequence of the larger efficacy of ozone (=1.4) compared to CO_2 (=1) (see Sect. 2.2.5). In 2100 the difference between the temperature change caused by CO_2 and ozone (as well as ozone plus methane) is less than 50%, although the radiative forcing of CO_2 is 3 and 5 times larger than for ozone and the sum of ozone plus methane, respectively. Only at steady-state (year 2250) the climate impact of CO_2 emissions clearly dominates over NO_x emissions.

**Climate impact
assessment tool:
AirClim**V. Grewe and A. Stenke

Title Page

Abstract

Introduction

Conclusions

References

Tables

Figures

◀

▶

◀

▶

Back

Close

Full Screen / Esc

Printer-friendly Version

Interactive Discussion

Therefore, although CO₂ emissions have a much larger atmospheric residence time, its climate impact in terms of near surface temperature changes is of comparable size to that of NO_x emissions via ozone formation and methane loss. A reduction of the NO_x emission index by 40% between 2000 and 2050, which will result in an emission index of 6 g(NO₂) per kg fuel as e.g. discussed as an option for future technology (Ponater et al., 2006) is shown by green boxes. This reduction will lower the importance of NO_x emissions. Still the temperature change induced by the NO_x emissions will not be negligible.

5.2 Supersonic air traffic and mitigation options: SCENIC

Figure 9b shows the temporal evolution of near surface temperature changes for a replacement of 500 subsonic aircraft by supersonics. A detailed discussion of the impact of such a replacement is given in Grewe et al. (2007). They applied 4 atmosphere-chemistry models (including E39/C) to investigate the climate impact and the impact on ultraviolet radiation for different options of a supersonic fleet.

Figure 9b shows the same main features as Fig. 9a in Grewe et al. (2007). Water vapour is the main contributor to climate change with regard to a supersonic fleet. Differences occur with respect to ozone since the mean value among 4 applied atmosphere-chemistry models was negative in Grewe et al. (2007), whereas here we calculate a small positive value. The turn around point between ozone increase at lower levels and ozone depletion at higher altitudes for a specific NO_x emission is still a major uncertainty (Grewe et al., 2007). Wuebbles et al. (2004) investigated the impact of the emission altitude on ozone column with a two-dimensional model and found a turnaround point between 13 km and 15 km, whereas E39/C simulates it around 14.5 km and 16.5 km. Currently, we are not able to include this uncertainty in AirClim. However, for the future one could include it, if multiple input data, precalculated by different models were used (see Sect. 2.2).

In the study by Grewe et al. (2007), E39/C was one of the applied models. However it was only applied to one of the options for computational reasons. Since AirClim is

**Climate impact
assessment tool:
AirClim**

V. Grewe and A. Stenke

Title Page

Abstract

Introduction

Conclusions

References

Tables

Figures

◀

▶

◀

▶

Back

Close

Full Screen / Esc

Printer-friendly Version

Interactive Discussion

numerically efficient, it can be applied to all of the scenarios, i.e. a higher NO_x emission index (P2), a doubling of the fleet size (P3), a decreased speed from Mach 2 to Mach 1.6 (P4), an increased range (P5), and a decreased cruise altitude (P6). Figure 11 is the analogous figure to their Figure 10 showing the impact of these options as a relative change with respect to the base case mixed fleet scenario (S5). The metrics near surface temperature change (blue filled bars) and ozone depletion (blue dashed bars) are taken into account. Since the options do not account for the same supersonic transport volume, we additionally normalised the results to the same supersonic transport volume (red bars). The product of the two metrics is then given as an overall metric (green bars).

In principle, the results lead to the same conclusions as in Grewe et al. (2007), i.e. the scenarios P6 (cruise altitude) and P4 (speed) show the smallest environmental impact. Differences occur especially in the calculated temperature change caused by an increased emission index of NO_x (P2) and increased range (P5). Note, that the errorbars express different ranges of uncertainty in Fig. 10 in Grewe et al. (2007) and our Fig. 11. Grewe et al. (2007) include, whenever possible, uncertainties covered by the range of model results, whereas in AirClim this uncertainty cannot be estimated, since only E39/C has been applied to derive the precalculated input data (Sect. 2.2). Differences are still within the range of uncertainty indicated by these errorbars, except for P5 and P6. The temperature increase derived for scenario P5 and the ozone depletion in scenario P6 significantly differs between the two approaches. The main difference between the findings for P5 and P6 and all other scenarios is that those results are only obtained by one model (SLIMCAT). Therefore, the results are somehow biased towards this model. An uncertainty range for ozone depletion could not be provided in Grewe et al. (2007) for the same reasons. Anyway, the main conclusion indicated by their results is the same.

The SCENIC scenarios discussed above are not suitable for a direct intercomparison of a subsonic and supersonic aircraft, since the impact of the replaced subsonic cannot be evaluated. Therefore an additional scenario (S4core) has been calculated

**Climate impact
assessment tool:
AirClim**

V. Grewe and A. Stenke

Title Page

Abstract

Introduction

Conclusions

References

Tables

Figures

◀

▶

◀

▶

Back

Close

Full Screen / Esc

Printer-friendly Version

Interactive Discussion

which includes only those subsonic aircraft, which are not replaced by supersonics in the mixed fleet scenario (Egelhofer, personal communication). Hence the difference between S4 and S4core and the difference between S5 and S4core refers to aircraft with the same characteristics and transport volume.

Figure 12 shows the direct intercomparison between those subsonic and supersonic aircraft, i.e. the impact of scenario S4 minus S4core (crossed) and the impact of scenario S5 minus S4core (filled). The results clearly show that the total climate impact of supersonics is approximately 5 times of that from subsonic aircraft. The fuel consumption for the subsonics, which are replaced is around 20 Tg/year compared to 60 Tg/year for the supersonics. This well explains the radiative forcing and temperature changes with respect to CO₂. The large difference in near surface temperature change arises predominantly from large water vapour changes, which are a consequence of the high emission altitude and the longer atmospheric residence times.

6 Conclusions

In this study we have proposed a methodology to assess the climate impact of emissions from air traffic. The main climate agents with respect to super- and subsonic air traffic are CO₂, H₂O, O₃, CH₄, and contrails. The functional chain from emissions to climate change of these species is complex and includes transport, chemistry, microphysics, and radiation. We have shown that the linearisation of these processes is possible and can be used within a more simple climate assessment tool, which facilitates the numerical efficient conversion of emission datasets into a metric of climate change. Here we propose near surface temperature changes in 2100 as a metric.

In order to linearise a complex climate-chemistry model (here: E39/C) we performed simulations applying a number of idealised emission scenarios. The results of these scenarios give insights into the atmospheric response, in terms of radiative forcing and temperature change to normalised emissions. Water vapour emissions show an increasing climate impact the higher or the closer to the tropics the emissions oc-

**Climate impact
assessment tool:
AirClim**

V. Grewe and A. Stenke

Title Page

Abstract

Introduction

Conclusions

References

Tables

Figures

◀

▶

◀

▶

Back

Close

Full Screen / Esc

Printer-friendly Version

Interactive Discussion

cur. Ozone from NO_x emissions has the largest warming potential at tropical latitudes around 100 to 200 hPa. Methane reduction caused by NO_x emissions is included. Although methane tends to reduce the warming and although atmospheric residence times are larger than those for ozone the overall effect of NO_x emissions is still one of a warming. The NO_x effect is reversed at high supersonic cruise levels, where NO_x leads to ozone depletion.

[Stevenson et al. \(2004\)](#) suggested that the integrated ozone radiative forcing could be outweighed by the methane impact when regarding short-term pulse emissions. In our study we find a significant reduction by approximately 50% of the near surface temperature response. The differences are to some extent arising from the larger ozone climate sensitivity, which is not taken into account in [Stevenson et al. \(2004\)](#), since they concentrated on radiative forcing, whereas we were focusing on near surface temperature changes.

Similar approaches to calculate the temperature changes caused by air traffic emissions have been used previously ([Sausen and Schumann, 2000](#); [Ponater et al., 2006](#); [Ling et al., 2006](#); [Lukachko et al., 2006](#); [Grewe et al., 2007](#)). They are all based on the same relationship between radiative forcing and temperature. Here we revised those methods with two main characteristics. First, the calculation of the radiative forcing for a specific emission dataset is included in the AirClim model by linearising these processes instead of precalculating them with detailed climate-chemistry models. Hence the place of the emission as well as its strength plays a key role in the determination of the radiative forcing. Second, we introduced typical residence times for stratospheric and tropospheric perturbations and for methane. With this, each regarded species has a typical residence time, which is perturbed by the air traffic emissions. Hence, the temporal development of ozone and methane perturbations differ remarkably in contrast to earlier studies.

The results performed for a subsonic fleet (TRADEOFF, SCENIC) show good agreement with previously calculated values for radiative forcing ([Sausen et al., 2005](#)). The calculated temperature change clearly shows that in future, e.g. 2100, CO_2 becomes

**Climate impact
assessment tool:
AirClim**V. Grewe and A. Stenke

Title Page

Abstract

Introduction

Conclusions

References

Tables

Figures

◀

▶

◀

▶

Back

Close

Full Screen / Esc

Printer-friendly Version

Interactive Discussion

the most important contributor to air traffic induced climate change, however NO_x emissions closely follow even when taking counteracting methane responses into account and also some challenging reductions in the emission index of NO_x . The regarded scenario assumes a constant fleet after 2050, which is probably unrealistic, but reasonable to illustrate the response to a steady-state. Assuming a further increase would even increase the importance of ozone compared to CO_2 , because the short-term effects from the increase in ozone due to an increase in air traffic and emissions dominate over long-term effects resulting from increasing CO_2 concentrations due to its long lifetime. This applies as long as air traffic increases considerably. That implies that all future measures for climate stabilisation should concentrate on both CO_2 and NO_x emissions.

Because of an extension to the SCENIC database we were able to directly compare subsonic and supersonic aircraft, in the sense that transport volume is the same and aircraft themselves are comparable. Such a comparison has not been performed so far (IPCC, 1999; Grewe et al., 2007). Instead, the impacts of a whole mixed fleet have been compared to a whole subsonic fleet. Our results show that supersonic aircraft of this size (250 passenger, 5400 nm range) have a five times larger climate impact than their subsonic counterpart. Smaller supersonic jets, e.g. business jets (e.g. 8 passenger 3500 nm) are also likely to have a larger climate impact than their subsonic counterparts. However, the enhancement is probably less than for larger aircraft, since one of the driving parameters for the enhancement of climate impact is the cruise altitude difference between subsonic and supersonic aircraft. Subsonic business jets already tend to fly at a higher altitudes than regular passenger aircraft to prevent a disturbance of air traffic. Therefore the differences in cruise altitude between sub- and supersonic business jets are expected to be smaller than for passenger aircraft.

Acknowledgements. This study has been partly supported by the European Commission through the Integrated Project HISAC and the Network of Excellence ECATS under the 6th Framework Programme. Many thanks to R. Egelhofer, Technical University Munich and C. Marizy, Airbus for providing additional and more detailed datasets of the SCENIC database and

**Climate impact
assessment tool:
AirClim**V. Grewe and A. Stenke

Title Page

Abstract

Introduction

Conclusions

References

Tables

Figures

◀

▶

◀

▶

Back

Close

Full Screen / Esc

Printer-friendly Version

Interactive Discussion

References

- Dameris, M., Grewe, V., Ponater, M., Deckert, R., Eyring, V., Mager, F., Matthes, S., Schnadt, C., Stenke, A., Steil, B., Brühl, C., and Giorgetta, M.: Long-term changes and variability in a transient simulation with a chemistry-climate model employing realistic forcing, *Atmos. Chem. Phys.*, 5, 2121–2145, 2005. [12190](#)
- Fuglestedt, J., Berntsen, T., Godal, O., Sausen, R., Shine, K., and Skodvin, T.: Metrics of climate change: Assessing radiative forcing and emission indices, *Clim. Change*, 58, 267–331, 2003. [12187](#)
- Grewe, V.: The origin of ozone, *Atmos. Chem. Phys.*, 6, 1495–1511, 2006. [12190](#)
- Grewe, V., Stenke, A., Ponater, M., Sausen, R., Pitari, G., Iachetti, D., Rogers, H., Dessens, O., Pyle, J., Isaksen, I., Gulstad, L., vde, O. S., Marizy, C., and Pascuillo, E.: Climate impact of supersonic air traffic: an approach to optimize a potential future supersonic fleet - Results from the EU-project SCENIC, *Atmos. Chem. Phys. Discuss.*, 7, 6143–6187, 2007. [12192](#), [12197](#), [12200](#), [12201](#), [12204](#), [12205](#), [12207](#), [12208](#), [12216](#)
- Hansen, J., Satoand, M., Ruedy, R., Nazarenko, L., Lacis, A., Schmidt, G., Russell, G., Aleinov, I., Bauer, M., Bauer, S., Bell, N., Cairns, B., Canuto, V., Chandler, M., Cheng, Y., DelGenio, A., Faluvegi, G., Fleming, E., Friend, A., Hall, T., Jackman, C., Kelley, M., Kiang, N., Koch, D., Lean, J., Lerner, J., Lo, K., Menon, S., Miller, R., Minnis, O., Novakov, T., Oinas, V., Perlwitz, J., Perlwitz, J., Rind, D., Romanou, A., Shindell, D., Stone, P., Sun, S., Tausnev, N., Tresher, D., Wielicki, B., Wong, T., and Zhang, S.: Efficacy of climate forcings, *J. Geophys. Res.*, 110, D18104, doi:10.1029/2005JD005776, 2005. [12192](#)
- Hein, R., Dameris, M., Schnadt, C., Land, C., Grewe, V., Köhler, I., Ponater, M., Sausen, R., Steil, B., Landgraf, J., and Brühl, C.: Results of an interactively coupled atmospheric chemistry-general circulation model: Comparison with observations, *Ann. Geophys.*, 19, 435–457, 2001. [12190](#)
- IPCC: Special report on aviation and the global atmosphere, Penner, J.E., Lister, D.H., Griggs, D.J., Dokken, D.J., McFarland, M. (eds.), Intergovernmental Panel on Climate Change, Cambridge University Press, New York, NY, USA, 1999. [12195](#), [12198](#), [12202](#), [12203](#), [12208](#)
- IPCC: Climate Change 2001 - The scientific basis. Contributions of working group I to the Third

**Climate impact
assessment tool:
AirClim**

V. Grewe and A. Stenke

Title Page

Abstract

Introduction

Conclusions

References

Tables

Figures

◀

▶

◀

▶

Back

Close

Full Screen / Esc

Printer-friendly Version

Interactive Discussion

Assessment Report of the Intergovernmental Panel of Climate Change (IPCC), Intergovernmental Panel on Climate Change, Cambridge University Press, New York, NY, USA, 2001. [12190](#), [12195](#)

Joshi, M., Shine, K., Ponater, M., Stuber, N., Sausen, R., and Li, L.: A comparison of climate response to different radiative forcings in three general circulation models: towards an improved metric of climate change, *Climate Dyn.*, 20, 843–854, 2003. [12192](#)

Land, C., Ponater, M., Sausen, R., and Roeckner, E.: The ECHAM4.L39(DLR) atmosphere GCM, Technical description and climatology, DLR-Forschungsbericht, 1991-31, 45 pp., ISSN 1434-8454, Deutsches Zentrum für Luft- und Raumfahrt, Köln, Germany, 1999.

Ling, L., Lee, D., and Sausen, R.: A climate response model for calculating aviation effects, IN: Book of abstracts, International Conference on Transport, Atmosphere and Climate 26–29 June 2006, Oxford, UK, <http://www.pa.op.dlr.de/tac>, 23, 2006. [12207](#)

Lukachko, S., Waitz, I., and Marais, M.: Valuing the Impact of Aviation on Climate, IN: Book of abstracts, International Conference on Transport, Atmosphere and Climate 26–29 June 2006, Oxford, UK, <http://www.pa.op.dlr.de/tac>, 24, 2006. [12207](#)

Manabe, S. and Strickler, R.: Thermal equilibrium of the atmosphere with a convective adjustment, *J. Atmos. Sci.*, 21, 361–385, 1964. [12196](#)

Ponater, M., Marquart, S., and Sausen, R.: Contrails in a comprehensive global climate model: Parameterisation and radiative forcing results, *J. Geophys. Res.*, 107, 4164, doi:10.1029/2001JD000429, 2002. [12191](#)

Ponater, M., Marquart, S., Sausen, R., and Schumann, U.: On contrail climate sensitivity, *Geophys. Res. Lett.*, 32, L10706, doi:10.1029/2005GL022580, 2005. [12192](#)

Ponater, M., Pechtl, S., Sausen, R., Schumann, U., and Hüttig, G.: Potential of the cryoplane technology to reduce aircraft climate impact: A state-of-the-art assessment, *Atmospheric Environment*, 40, 6928–6944, doi:10.1016/j.atmosenv.2006.06.036, 2006. [12192](#), [12204](#), [12207](#)

Reithmeier, C. and Sausen, R.: ATTILA - Atmospheric Tracer Transport in a Lagrangian Model, *Tellus Series B - Chemical and Physical Meteorology*, 54, 278–299, 2002.

Sausen, R. and Schumann, U.: Estimates of the climate response to aircraft CO₂ and NO_x emissions scenarios, *Clim. Change*, 44, 25–58, 2000. [12187](#), [12188](#), [12196](#), [12207](#)

Sausen, R., Gierens, K., Ponater, M., and Schumann, U.: A diagnostic study of the global distribution of contrails, Part I: present day climate, *Theor. Appl. Climatol.*, 61, 127–141, 1998. [12191](#)

ACPD

7, 12185–12229, 2007

**Climate impact
assessment tool:
AirClim**

V. Grewe and A. Stenke

Title Page

Abstract

Introduction

Conclusions

References

Tables

Figures

◀

▶

◀

▶

Back

Close

Full Screen / Esc

Printer-friendly Version

Interactive Discussion

EGU

- Sausen, R., Isaksen, I., Grewe, V., Hauglustaine, D., Lee, D. S., Myhre, G., Köhler, M. O., Pitari, G., Schumann, U., Stordal, F., and Zerefos, C.: Aviation Radiative Forcing in 2000: An Update on IPCC (1999), *Meteorol. Z.*, 14, 555–561, 2005. [12202](#), [12203](#), [12207](#), [12217](#)
- Schumann, U., Busen, R., and Plohr, M.: Experimental test of the influence of propulsion efficiency on contrail formation, *J. Aircraft*, 37, 1083–1087, 2000. [12187](#)
- Shine, K., Berntsen, T., Fuglestvedt, J., and Sausen, R.: Scientific issues in the design of metrics for inclusion of oxides of nitrogen in global climate agreements, *PNAS*, 44, 15768–15773, 2005. [12187](#)
- Steil, B., Dameris, M., Brühl, C., Crutzen, P., Grewe, V., Ponater, M., and Sausen, R.: Development of a Chemistry Module for GCMs: First Results of a Multiannual Integration, *Ann. Geophys.*, 16, 205–228, 1998. [12190](#)
- Stevenson, D., Doherty, R., Sanderson, M., Collins, W., Johnson, C., and Derwent, R.: Radiative forcing from aircraft NO_x emissions: Mechanisms and seasonal dependence, *J. Geophys. Res.*, 109, D17307, doi:10.1029/2004JD004759, 2004. [12207](#)
- Stuber, N., Sausen, R., and Ponater, M.: Stratosphere adjusted radiative forcing calculations in a comprehensive climate model, *Theor. Appl. Climatol.*, 68, 125–135, 2001. [12192](#)
- Wuebbles, D., Dutta, M., Patten, K., and Baughcum, S.: Parametric study of potential effects of aircraft emissions on stratospheric ozone, *Proceedings of the AAC-Conference*, July 2003, Friedrichshafen, Germany, edited by: Sausen, R., Fichter, C., and Amanatidis, G., 140–144, 2004. [12204](#)

**Climate impact
assessment tool:
AirClim**

V. Grewe and A. Stenke

Title Page

Abstract

Introduction

Conclusions

References

Tables

Figures

◀

▶

◀

▶

Back

Close

Full Screen / Esc

Printer-friendly Version

Interactive Discussion

**Climate impact
assessment tool:
AirClim**

V. Grewe and A. Stenke

Table 1. Pressure levels (P_{id}) in [hPa] of idealised emission scenarios.

P_{id}	Description	Abbr.
52	Supersonic Cruise Level - High	SSCL-H
89	Supersonic Cruise Level – Medium	SSCL-M
132	Supersonic Cruise Level – Low	SSCL-L
198	Subsonic Cruise Level	SubCL
499	Climb High	Climb-H
967	Climb Low	Climb-L

Title Page

Abstract

Introduction

Conclusions

References

Tables

Figures

◀

▶

◀

▶

Back

Close

Full Screen / Esc

Printer-friendly Version

Interactive Discussion

**Climate impact
assessment tool:
AirClim**

V. Grewe and A. Stenke

Table 2. Latitudinal regions of idealised emission scenarios.

Latitude bands	Lat _{i,d}	Description	Abbreviation
60° N–90° N	75° N	Northern high latitudes	Pole
30° N–60° N	45° N	Northern mid-latitudes	MidLat
30° S–30° N	0°	Tropical region	Tropic
45° S–30° S	37.5° S	Southern mid-latitudes	South

Title Page

Abstract

Introduction

Conclusions

References

Tables

Figures

◀

▶

◀

▶

Back

Close

Full Screen / Esc

Printer-friendly Version

Interactive Discussion

**Climate impact
assessment tool:
AirClim**

V. Grewe and A. Stenke

Title Page

Abstract

Introduction

Conclusions

References

Tables

Figures

I ◀

▶ I

◀

▶

Back

Close

Full Screen / Esc

Printer-friendly Version

Interactive Discussion

Table 3. Emission strength of idealised scenarios.

species	Emission [10^{-15} kg/kg/s]
Fuel	F=100
H ₂ O	H=125
NO _x	N=0.45

**Climate impact
assessment tool:
AirClim**

V. Grewe and A. Stenke

Table 4. Short description of the applied aircraft emission datasets.

Project	Abbr.	Year	Description	Fuel [Tg/a]	EI(NO _x)
TRADEOFF		2000	Subsonic air traffic	169	12.78
SCENIC	S2	2025	Subsonic air traffic	393	12.97
SCENIC	S4	2050	Subsonic air traffic	677	10.85
SCENIC	S3	2025	Mixed fleet	393	12.42
SCENIC	S5	2050	Mixed fleet	721	10.33
SCENIC	S4core	2050	Subsonic w/o a/c to be replaced	659	10.85

Title Page

Abstract

Introduction

Conclusions

References

Tables

Figures

◀

▶

◀

▶

Back

Close

Full Screen / Esc

Printer-friendly Version

Interactive Discussion

**Climate impact
assessment tool:
AirClim**

V. Grewe and A. Stenke

Table 5. Radiative forcing [mW/m^2] of various climate agents calculated with the climate-chemistry model E39/C (from Grewe et al., 2007) and the linearised model AirClim for the difference in the scenario S5 minus S4, i.e. mixed super- and subsonic fleet minus subsonic fleet for the year 2050.

	H ₂ O	O ₃	CH ₄	Contrails	Total
E39/C	17.7	0.3	-0.5	-0.6	16.9
AirClim	17.3	0.2	-0.8	-0.4	16.3

Title Page

Abstract

Introduction

Conclusions

References

Tables

Figures

I◀

▶I

◀

▶

Back

Close

Full Screen / Esc

Printer-friendly Version

Interactive Discussion

Climate impact assessment tool: AirClim

V. Grewe and A. Stenke

Title Page

Abstract

Introduction

Conclusions

References

Tables

Figures

◀

▶

◀

▶

Back

Close

Full Screen / Esc

Printer-friendly Version

Interactive Discussion

Table 6. Radiative forcing [mW/m^2] of various climate agents calculated by Sausen et al. (2005) and by applying the linearised model AirClim for TRADEOFF emission data. *The sum differs slightly from the total value in Sausen et al. (2005), because soot and sulphate contributions to radiative forcing are omitted. Note also that contrail-cirrus effects are not included due to lack of knowledge.

	CO ₂	H ₂ O	O ₃	CH ₄	Contrails	Sum*
Sausen et al.	25.3	2.0	21.9	−10.4	10.0	48.8*
AirClim	22.8	2.6	15.4	−3.3	10.9	48.4

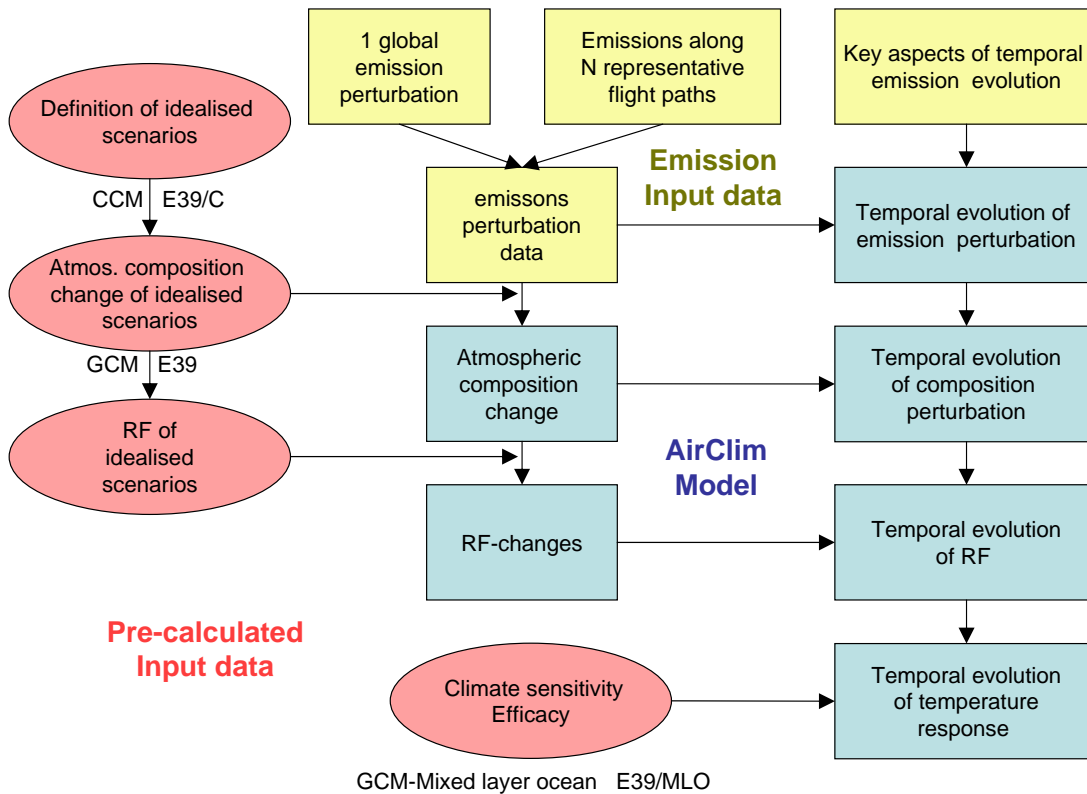


Fig. 1. Overview of the multi-step approach to derive near surface temperature changes and ozone depletion from emission scenarios.

Climate impact assessment tool: AirClim

V. Grewe and A. Stenke

Title Page

Abstract

Introduction

Conclusions

References

Tables

Figures

◀

▶

◀

▶

Back

Close

Full Screen / Esc

Printer-friendly Version

Interactive Discussion

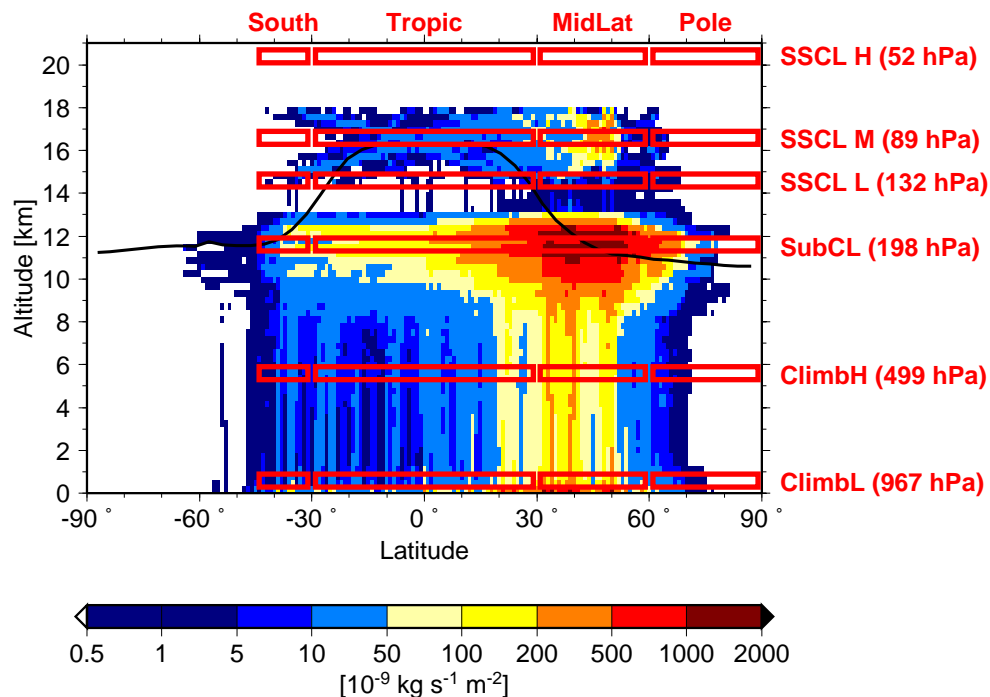


Fig. 2. Location of 24 emission regions used for the linearisation of perturbations of the atmospheric composition. Fuel consumption (zonally integrated) of a mixed fleet (SCENIC 2050 data) is underlaid for illustration [kg/s/m^2].

Climate impact assessment tool: AirClim

V. Grewe and A. Stenke

Title Page

Abstract

Introduction

Conclusions

References

Tables

Figures

◀

▶

◀

▶

Back

Close

Full Screen / Esc

Printer-friendly Version

Interactive Discussion

Climate impact assessment tool: AirClim

V. Grewe and A. Stenke

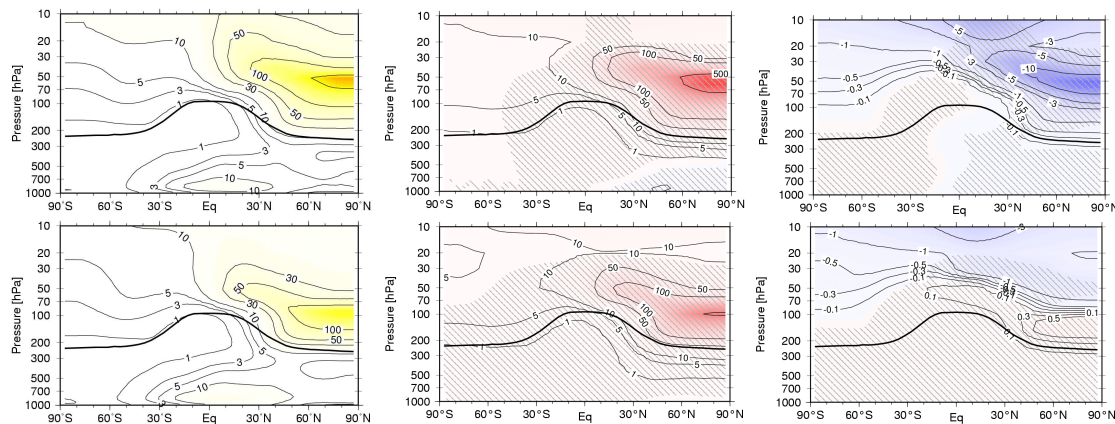


Fig. 3. Annual mean changes in zonal mean water vapour (left) [ppbv], nitrogen oxides (NO_y) (mid) [pptv], and ozone (right) [ppbv] for polar emissions at high (top) and mid (bottom) super-sonic cruise levels. Water vapour changes are all significant at a 95% level; significant changes are hatched for other species. The thick black line indicates the thermal tropopause.

Title Page

Abstract

Introduction

Conclusions

References

Tables

Figures

◀

▶

◀

▶

Back

Close

Full Screen / Esc

Printer-friendly Version

Interactive Discussion

**Climate impact
assessment tool:
AirClim**

V. Grewe and A. Stenke

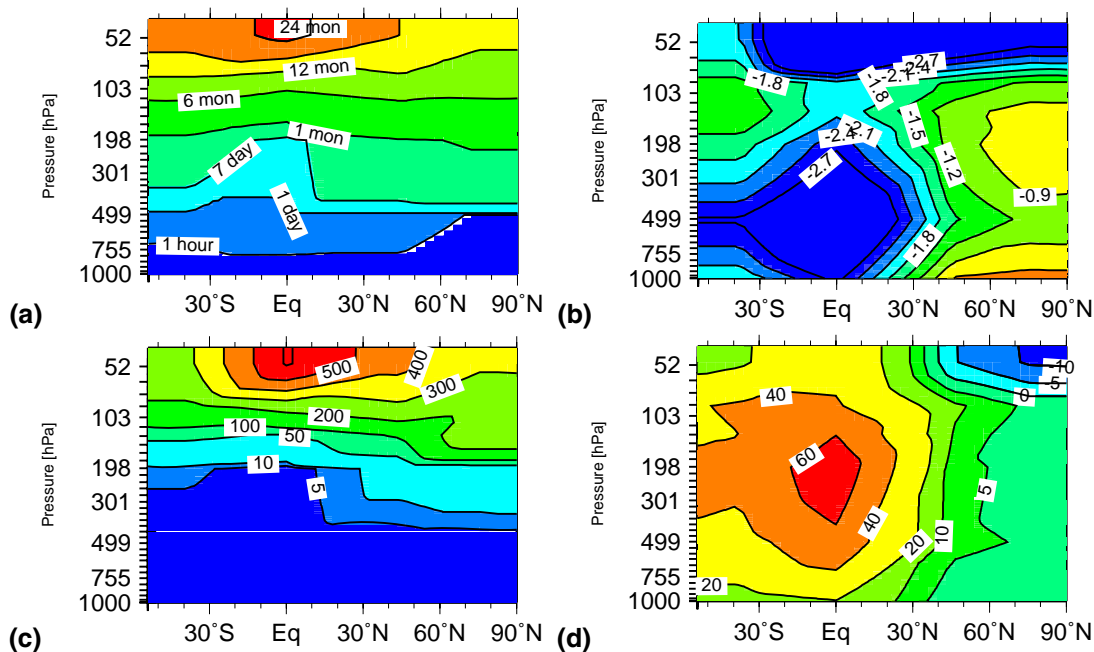


Fig. 4. Water vapour perturbation lifetime **(a)**, methane lifetime change [%] **(b)**, and radiative forcing at the tropopause for the water vapour **(c)** and ozone perturbations **(d)** normalised to the same total emission of 1 Pg water vapour and 1 TgN of NO_y in mW/m^2 . Altitude and latitude indicates the region of the idealised emissions.

Full Screen / Esc

Printer-friendly Version

Interactive Discussion

**Climate impact
assessment tool:
AirClim**

V. Grewe and A. Stenke

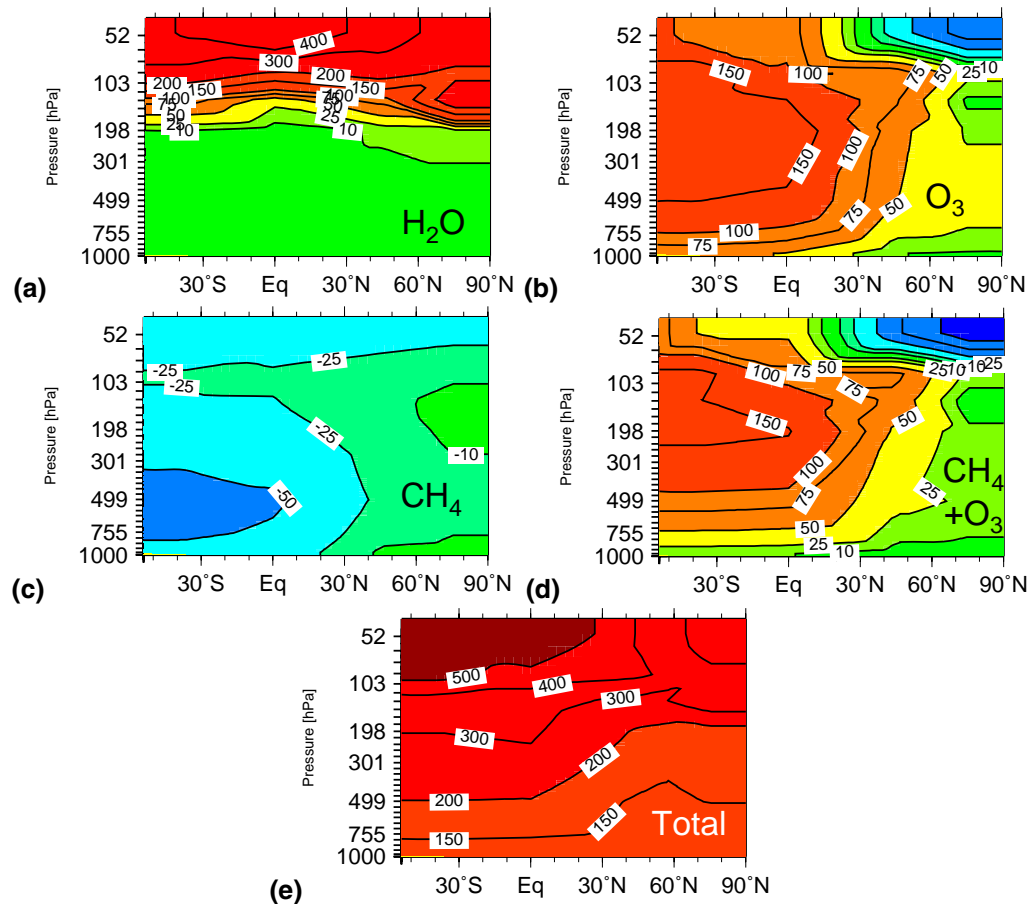


Fig. 5. Near surface temperature changes [mK] in 2100 as a function of latitude and altitude of the emissions for (a) H_2O (b) O_3 (c) CH_4 (d) $\text{O}_3 + \text{CH}_4$ (e) Total. The emissions are normalised to the totals of scenario S4, i.e. subsonic air traffic for 2050.

Title Page

Abstract

Introduction

Conclusions

References

Tables

Figures

◀

▶

◀

▶

Back

Close

Full Screen / Esc

Printer-friendly Version

Interactive Discussion

**Climate impact
assessment tool:
AirClim**

V. Grewe and A. Stenke

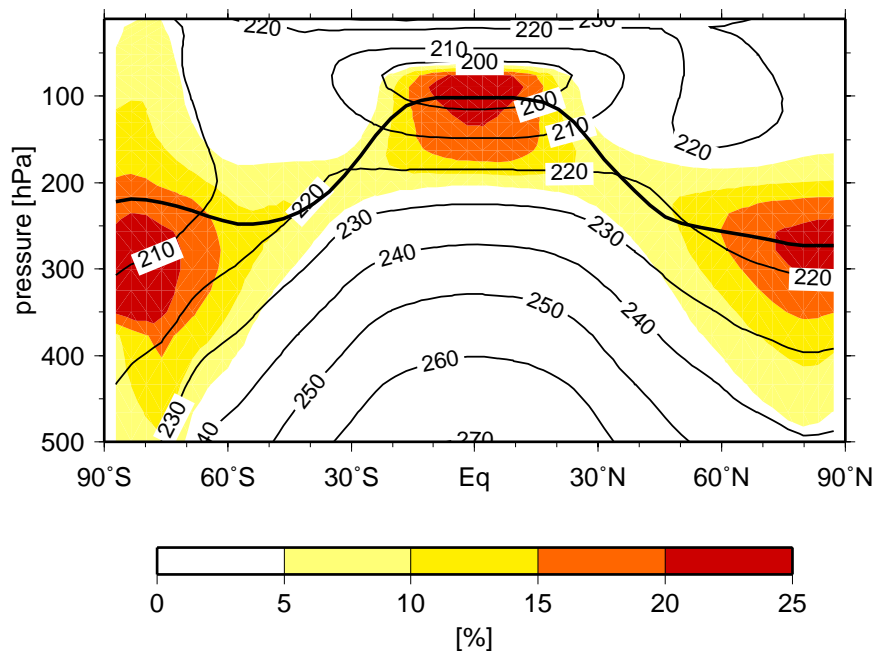


Fig. 6. Annual mean potential contrail coverage [%] for 2050 (colour pattern). Thin lines show annual mean temperatures [K] and the thick line shows the location of the tropopause.

[Title Page](#)[Abstract](#)[Introduction](#)[Conclusions](#)[References](#)[Tables](#)[Figures](#)[◀](#)[▶](#)[◀](#)[▶](#)[Back](#)[Close](#)[Full Screen / Esc](#)[Printer-friendly Version](#)[Interactive Discussion](#)

**Climate impact
assessment tool:
AirClim**

V. Grewe and A. Stenke

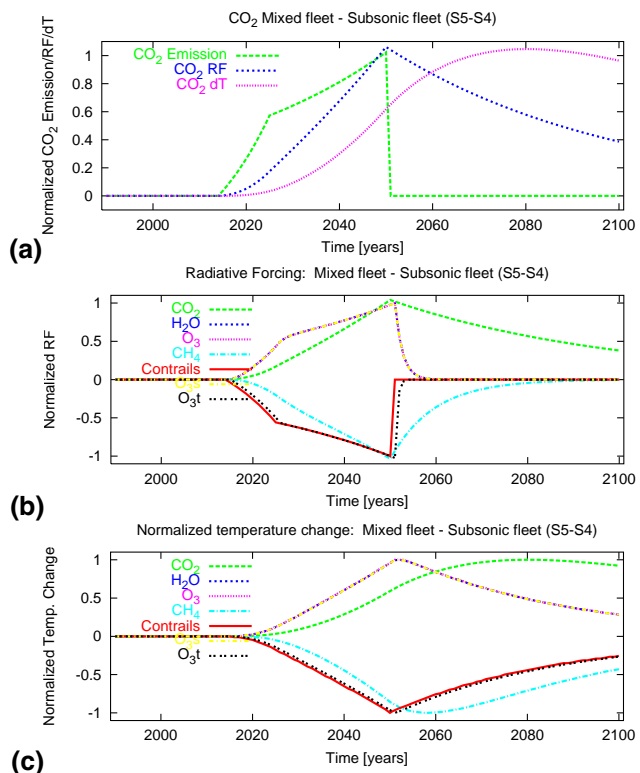


Fig. 7. Nondimensional temporal development of **(a)** CO₂ emissions **(b)** radiative forcing and **(c)** temperature for a supersonic fleet (here: SCENIC S5 mixed fleet minus subsonic fleet S4). Emissions are switched off from 2050 onwards to illustrate decay times. All curves are normalised to 1 for their maximum values to illustrate the behaviour of each species. Ozone is splitted into a stratospheric (O₃s) and tropospheric part (O₃t). Curves for water vapour, ozone and stratospheric ozone are overlaid.

Title Page

Abstract

Introduction

Conclusions

References

Tables

Figures

◀

▶

◀

▶

Back

Close

Full Screen / Esc

Printer-friendly Version

Interactive Discussion

Climate impact assessment tool: AirClim

V. Grewe and A. Stenke

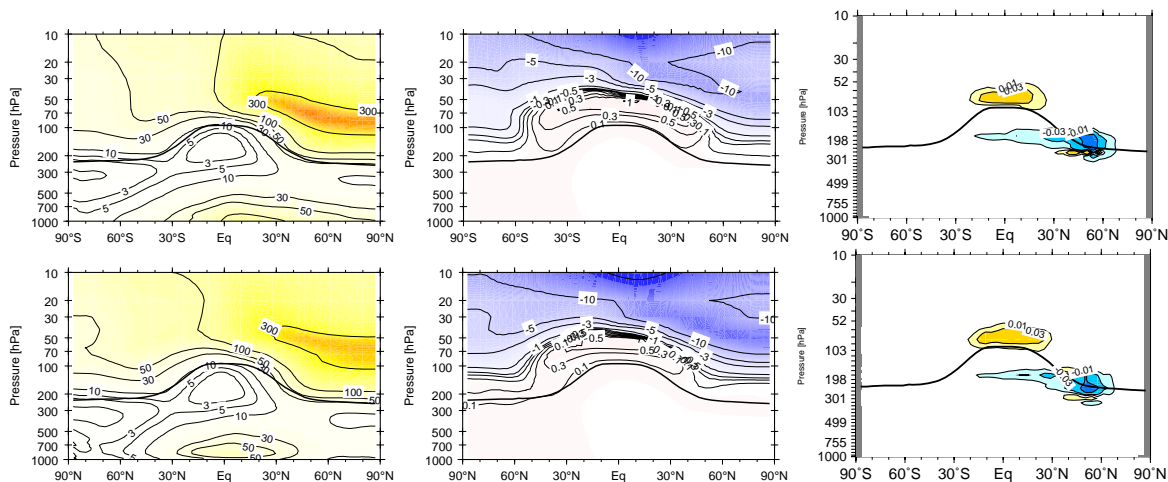


Fig. 8. Annual mean changes in water vapour (left) [ppbv], ozone (mid) [ppbv], and contrail coverage (right) [0.1%] caused by a supersonic fleet (here: SCENIC S5 mixed fleet minus subsonic fleet S4). Top: Results derived with E39/C; Bottom: Calculated with AirClim. Thick lines indicates the location of the tropopause. Isolines for contrail changes are -0.3 , -0.1 , -0.03 , -0.01 , 0.01 , 0.03 , 0.1 , 0.3 .

Title Page

Abstract

Introduction

Conclusions

References

Tables

Figures

◀

▶

◀

▶

Back

Close

Full Screen / Esc

Printer-friendly Version

Interactive Discussion

**Climate impact
assessment tool:
AirClim**

V. Grewe and A. Stenke

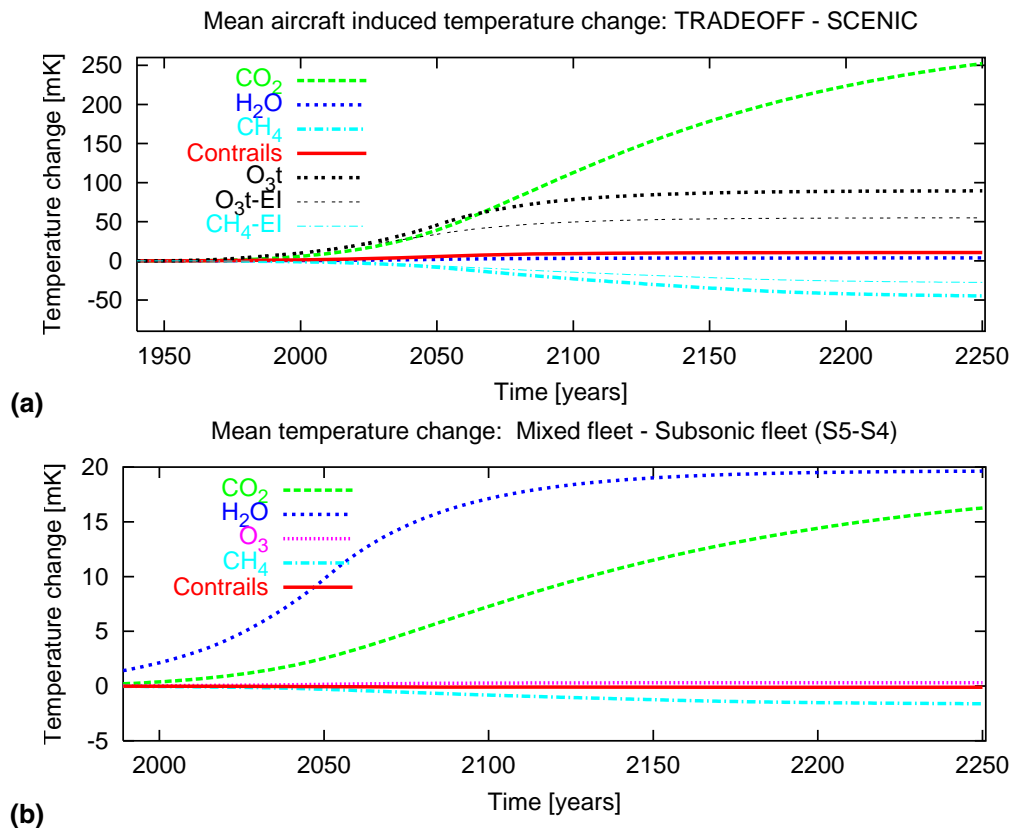


Fig. 9. Temporal development of temperature changes [mK] due to aircraft emissions for **(a)** subsonic air traffic (TRADEOFF and SCENIC); **(b)** supersonic transport (mixed fleet minus subsonic fleet; SCENIC) as calculated with AirClim. The extension EI indicates a scenario with a reduction of the emission index of NO_x by 40%.

Title Page

Abstract

Introduction

Conclusions

References

Tables

Figures

◀

▶

◀

▶

Back

Close

Full Screen / Esc

Printer-friendly Version

Interactive Discussion

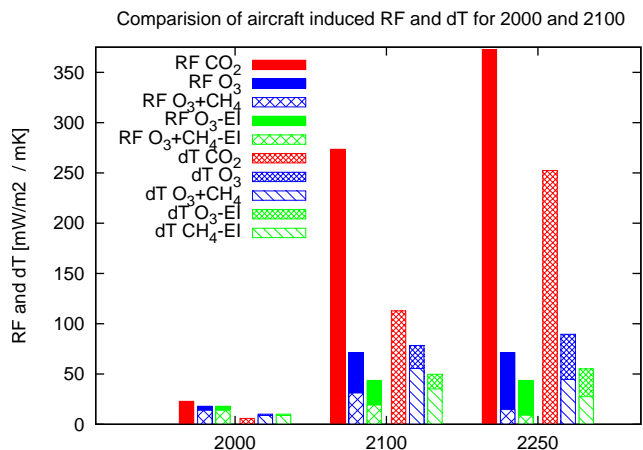


Fig. 10. Intercomparison of the importance of subsonic air traffic CO₂ (red) versus NO_x (blue) emissions for climate change. Left three bars indicate radiative forcing and right three bars temperature change for each year. A scenario including a reduction of the NO_x emission index by 40% from 2000 to 2050 is included (green). The bar for NO_x include ozone (whole bar) and ozone+methane (reduced bar) changes. The extension EI indicates a scenario with a reduction of the emission index of NO_x by 40%.

Climate impact assessment tool: AirClim

V. Grewe and A. Stenke

Title Page

Abstract

Introduction

Conclusions

References

Tables

Figures

◀

▶

◀

▶

Back

Close

Full Screen / Esc

Printer-friendly Version

Interactive Discussion

Climate impact assessment tool: AirClim

V. Grewe and A. Stenke

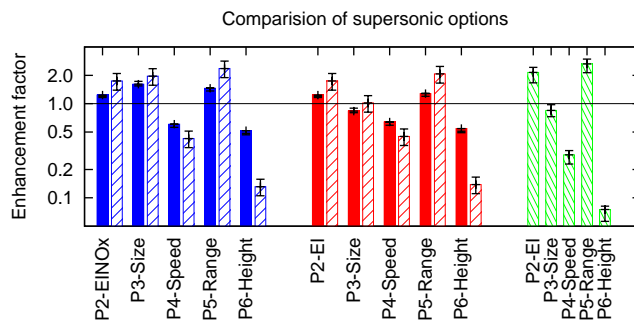


Fig. 11. Relative changes in near surface temperature for the year 2100 (solid bars) and for ozone (dashed bars) with respect to the impact of a supersonic base case scenario (SCENIC scenario S5 minus S4). Changes are given for constant transport volume of the total fleet (blue) and constant supersonic transport volume (red). The product of both factors is added (green) as an overall metric. For each bar an uncertainty range is given, which represents minimum and maximum values. The larger the enhancement factor the larger is the respective impact on climate and ozone. The calculations are performed with AirClim.

Title Page

Abstract

Introduction

Conclusions

References

Tables

Figures

◀

▶

◀

▶

Back

Close

Full Screen / Esc

Printer-friendly Version

Interactive Discussion

Climate impact assessment tool: AirClim

V. Grewe and A. Stenke

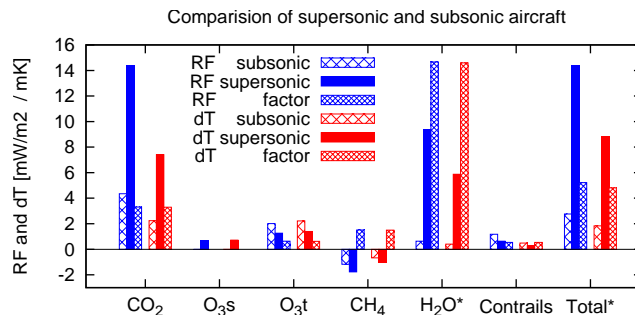


Fig. 12. Intercomparison of the near surface temperature change caused by supersonic (filled) aircraft and the respective (replaced) subsonic aircraft (dashed) for 2100. The third column in each group indicates the factor between the supersonic and subsonic impact. Ozone is splitted into the stratospheric (O_{3s}) and tropospheric (O_{3t}) contribution. *Values of RF and temperature changes are divided by 3 for presentability reasons.

Title Page

Abstract

Introduction

Conclusions

References

Tables

Figures

◀

▶

◀

▶

Back

Close

Full Screen / Esc

Printer-friendly Version

Interactive Discussion